Distribution of Ohm k from the scale-factor cutoff measure

PHYSICAL REVIEW D **81,** 083527 (2010)

Distribution of Ω_k from the scale-factor cutoff measure

Andrea De Simone[1] and Michael P. Salem[2]

[1]*Center for Theoretical Physics, Laboratory for Nuclear Science, and Department of Physics, Massachusetts Institute of Technology, Cambridge, Massachusetts 02139, USA*

[2]*Institute of Cosmology, Department of Physics and Astronomy, Tufts University, Medford, Massachusetts 02155, USA*

(Received 13 January 2010; published 22 April 2010)

Our Universe may be contained in one among a diverging number of bubbles that nucleate within an eternally inflating multiverse. A promising measure to regulate the diverging spacetime volume of such a multiverse is the scale-factor cutoff, one feature of which is bubbles are not rewarded for having a longer duration of slow-roll inflation. Thus, depending on the landscape distribution of the number of e-folds of inflation among bubbles like ours, we might hope to measure spatial curvature. We study a recently proposed cartoon model of inflation in the landscape and find a reasonable chance (about 10%) that the curvature in our Universe is well above the value expected from cosmic variance. Anthropic selection does not strongly select for curvature as small as is observed (relative somewhat larger values), meaning the observational bound on curvature can be used to rule out landscape models that typically give too little inflation.

DOI: 10.1103/PhysRevD.81.083527 PACS numbers: 98.80.Cq

I. INTRODUCTION

Inflation is generically eternal, with the physical volume of false-vacuum inflating regions increasing exponentially with time and ''pocket universes'' like ours constantly nucleating out of the false vacuum. Each of these pockets contains an infinite, open Friedmann-Robertson-Walker (FRW) universe and, when the fundamental theory admits a landscape of meta-stable vacua, each may contain different physical parameters, or even different fundamental physics, than those observed within our Universe. In order to make meaningful predictions on what physics we should expect to observe within our pocket it is necessary to adopt a prescription to regulate the diverging spacetime volume of the multiverse (for recent reviews, see, for example, Refs. [1–5]).

This issue, known as the measure problem, has been addressed in several different ways so far [6–23]. Different approaches, in general, make different observational predictions, and some of these apparently conflict with observation. For example, approaches that define probabilities with respect to a global proper-time foliation [6–9,17] suffer a ''youngness paradox,'' predicting that we should have evolved at a very early cosmic time, when the conditions for life were very hostile [24,25]. Volume-weighting measures, like the so-called ''gauge invariant'' or ''stationary'' measures [10,18,22] and the pocket-based measures [11–14], have a ''runaway inflation'' problem. These measures predict that we should observe severely large or small values of the primordial density contrast [26,27] and the gravitational constant [28], while these parameters appear to sit comfortably near the middle of their respective anthropic ranges [28,29]. (Some suggestions to possibly get around this issue have been described in Refs. [27,30].)

The causal patch measure [15,16] and the scale-factor cutoff measure [31,32] survive these hazards. Furthermore, under reasonable assumptions about the landscape [15,33], these measures do not suffer a ''Boltzmann brain invasion'' [34–40], where observers created as rare quantum fluctuations outnumber ''normal'' observers who evolve from out-of-equilibrium processes in the wake of the big bang. There is also encouraging evidence that these measures coincide with probability measures stemming from independent theoretical considerations [21,23]. Thus, we consider these measures to be promising proposals to regulate the diverging spacetime volume of the multiverse.

An interesting feature of these measures is that they do not reward regions of the multiverse for having longer periods of slow-roll inflation. Thus, one might hope that in our bubble slow-roll inflation did not last long enough to wash away all of the relics of the bubble-nucleation event. One such relic is the large geometric curvature of the bubble at the time of its nucleation. (Note that the large-curvature initial bubble is still homogeneous and isotropic, due to the symmetries of the eternally inflating vacuum in which it nucleates [41,42].) In this paper, we study the probability distribution of the curvature parameter Ω_k,

$$\Omega_k = 1 - \frac{8\pi G}{3H^2}\rho_{\rm total}, \tag{1}$$

where H is the Hubble parameter and $\rho_{\rm total}$ is the total energy density of our Universe.

For simplicity, we only focus on the scale-factor cutoff measure. The joint probability distribution for Ω_k and the cosmological constant, using the causal entropic principle [43], has been already investigated in Ref. [44]. The case of the causal patch measure was explored in Ref. [45]. The predictions of all these approaches turn out to be very similar.

We first study the effect of anthropic selection in favor of small Ω_k, which derives from the tendency of large curvature to inhibit structure formation. Anthropic distributions for the curvature parameter have previously been estimated by Vilenkin and Winitzki [46] and by Garriga, Tanaka, and Vilenkin [11]; however that work did not include a nonzero cosmological constant. The cosmological constant was included in a more recent calculation by Freivogel, Kleban, Rodriguez Martinez, and Susskind (FKRMS) [47]; however that work did not take into account the Gaussian distribution of primordial density perturbations, which allows for structure formation even when the curvature is large enough to prevent the collapse of a typical-amplitude density fluctuation. We provide a complete treatment of the problem, using updated cosmological data. Although anthropic selection strongly suppresses the probability to measure $\Omega_k > 0.6$ or so, by itself it does not strongly select for values of Ω_k as small as the present observational bound.

The curvature parameter today Ω_k^0 depends exponentially on the number of e-folds of slow-roll inflation N_e. The authors of Ref. [47] proposed a simple toy model of inflation in the landscape, for which they find N_e to follow the distribution $dP_0(N_e) \propto N_e^{-4} dN_e$. We adopt this model and use the scale-factor cutoff measure to predict the distribution of Ω_k among bubbles like ours in the multiverse. The result is essentially what one might guess by ignoring volume weighting, anthropic selection, and the effects of the measure. The predicted distribution of Ω_k prefers values below that expected from cosmic variance [48,49], but it gives reasonable hope for Ω_k to be significantly larger. Specifically, there is about a 6% chance to observe $\Omega_k^0 \geq 10^{-3}$ and about an 11% chance to observe $\Omega_k^0 \geq 10^{-4}$, the latter corresponding roughly to accuracy to which Ω_k can in principle be determined [49]. These predictions rely on some simple assumptions about inflation, including a reheating temperature of $T_* \approx 10^{15}$ GeV. (All else being equal, lowering the reheating temperature increases the likelihoods for these observations.)

To make the above predictions as precise as possible, we have assumed that Ω_k^0 is measured at the present cosmic time, and input the observational constraint $\Omega_k^0 \leq 0.013$ [50] (for simplicity we treat this 95% confidence level as a hard bound). Yet, related to the question of what we (observers living at the present cosmic time) expect to measure, there is the question of what typical observers (i.e. those living at arbitrary times) in bubbles like ours measure. To address this question it is convenient to work with a time-invariant measure of curvature; for this we choose

$$k = \left(\frac{\Omega_k^3}{\Omega_\Lambda \Omega_m^2}\right)^{1/3}, \tag{2}$$

which in effect expresses the inverse curvature radius squared, $r_{\rm curv}^{-2} = H^2 \Omega_k$, in units related to the late-time matter density and cosmological constant (here Ω_Λ is the density parameter of the cosmological constant; Ω_m is that of nonrelativistic matter). As before we restrict attention to bubbles just like ours, including the value of the cosmological constant, and times after nonrelativistic matter domination, when presumably all of the observers arise. One can then ask how typical is our measurement, $k \leq 0.035$. Using the scale-factor cutoff, we find that observers typically observe k to satisfy this bound.

Because anthropic selection is rather weak in the vicinity of the bound $k \leq 0.035$, we can rule out certain distributions of N_e, because they predict that we should measure k to be much larger than we do. The assumptions referred to above relate $k = 0.035$ to $N_e = 63.7$ e-folds of inflation. Although anthropic selection is weak for N_e near to and greater than this number, it becomes strong at $N_e \approx 61$. Thus, a landscape distribution of N_e can be ruled out if its weight over the interval $63.7 \leq N_e$ is much less than its weight over the interval $61 \lesssim N_e < 63.7$. Different assumptions about inflation (for example higher or lower reheating temperature) merely shift the numbers in these inequalities.

The remainder of this paper is organized as follows. In Sec. II, we review some background material that is relevant to our main calculation, including a brief description of the scale-factor cutoff measure (Sec. II A), a description of how one can model bubble geometry before and after slow-roll inflation (Sec. II B), and some background on structure formation in an open FRW universe (Sec. II C). The distribution of Ω_k is calculated in Sec. III. In Sec. IV we discuss anthropic considerations and describe how our results can be used to rule out hypothetical models of inflation in the landscape. The analysis of Secs. III and IV is discussed in the context of an alternative form of the scale-factor cutoff measure in Appendix A, where it is shown that the predictions are qualitatively unchanged. We draw our conclusions in Sec. V.

II. BACKGROUND

A. The scale-factor cutoff measure

Perhaps the simplest way to regulate the infinities of eternal inflation is to impose a cutoff on a hypersurface of constant global time [6–10]. One starts with a patch of a spacelike hypersurface Σ somewhere in an inflating region of spacetime, and follows its evolution along the congruence of geodesics orthogonal to Σ. The scale-factor time is defined as

$$t = \ln a, \tag{3}$$

where a is the expansion factor along the geodesics. The scale-factor time is related to the proper time τ by

$$dt = H d\tau, \tag{4}$$

where H is the Hubble expansion rate of the congruence. The spacetime region swept out by the congruence will typically expand to unlimited size, generating an infinite

number of pockets. (If the patch does not grow without limit, one chooses another initial patch Σ and starts again.) The resulting four-volume is infinite, but we cut it off at some fixed scale-factor time $t = t_c$. To find the relative probabilities of different events, one counts the numbers of such events in the finite spacetime volume between Σ and the $t = t_c$ hypersurface, and then takes the limit $t_c \to \infty$.

The term "scale factor" is often used in the context of homogeneous and isotropic geometries; yet on very large and on very small scales the multiverse may be very inhomogeneous. A simple way to deal with this is to take the factor H in Eq. (4) to be the local divergence of the four-velocity vector field along the congruence of geodesics orthogonal to Σ,

$$H(x) \equiv (1/3)u^{\mu}{}_{;\mu}. \tag{5}$$

When more than one geodesic passes through a point, the scale-factor time at that point may be taken to be the smallest value among the set of geodesics. In collapsing regions $H(x)$ is negative, in which case the corresponding geodesics are continued unless or until they hit a singularity.

This "local" definition of scale-factor time has a simple geometric meaning. The congruence of geodesics can be thought of as representing a "dust" of test particles scattered uniformly on the initial hypersurface Σ. As one moves along the geodesics, the density of the dust in the orthogonal plane decreases. The expansion factor a in Eq. (3) can then be defined as $a \propto \rho^{-1/3}$, where ρ is the density of the dust, and the cutoff is triggered when ρ drops below some specified level.

Although the local scale-factor time closely follows the FRW scale factor in expanding spacetimes—such as inflating regions and thermalized regions not long after reheating—it differs dramatically from the FRW scale factor as small-scale inhomogeneities develop during matter domination in universes like ours. In particular, the local scale-factor time nearly grinds to a halt in regions that have decoupled from the Hubble flow. It is not clear whether we should impose this particular cutoff, which would essentially include the entire lifetime of any nonlinear structure that forms before the cutoff, or impose a cutoff on some nonlocal time variable that more closely tracks the FRW scale factor.[1]

Note, however, that if we focus on an idealized multiverse composed entirely of thin-wall bubbles, in which bubble collisions do not significantly deform one of the involved bubbles, then it is possible to unambiguously define the FRW Hubble rate H at any point along the congruence. In particular, the initial FRW symmetry of each bubble defines a foliation over which the expansion rate (5) can be spatially averaged. Scale-factor time is continued from one bubble to another by taking it to be continuous across bubble walls. We emphasize that for more general landscapes, such a definition is not available. We leave to future work developing a nonlocal modification of the scale-factor time (5) that both approximates our intuitive notion of FRW averaging and also extends into more complicated geometries.

In general, the local scale-factor cutoff measure defined by (4) and (5) and the nonlocal scale-factor cutoff defined above make different predictions for physical observables. In the present case of the curvature parameter, however, the prediction of each choice is qualitatively the same. In the main body of this paper we refer to the above nonlocal definition of scale-factor time, for which we take the FRW scale factor as a suitable approximation. In Appendix A the analysis is briefly repeated using the local scale-factor time parametrization.

To facilitate further discussion, we here review some general features of eternally inflating spacetimes in light of a scale-factor time foliation. Regions of an eternally inflating multiverse might involve fields sitting in local potential minima, at least some of which correspond to positive false-vacuum energies. Evolution of the multiverse is then governed by bubble nucleation through quantum tunneling [51,52], either from one local minimum to another or from a local minimum to a region of classical slow-roll inflation.[2] In the latter case, the bubble interiors have the geometry of open FRW universes. Bubbles of interest to us here have a period of slow-roll inflation followed by reheating.

In the limit of large scale-factor time, the number of objects of any type that have formed prior to time t is (asymptotically) proportional to $e^{\gamma t}$, where γ is a universal constant. This universal asymptotic scaling behavior is a consequence of the physical volume of the multiverse being dominated by a subset of vacua, the "dominant" vacua, whose collective volume grows at a constant rate. This is the set of de Sitter vacua corresponding to the state with the smallest-magnitude eigenvalue in the master rate equation for the multiverse [56]. In many landscapes, there

[1]The distinction between these two forms of scale-factor time was first pointed out by Bousso, Freivogel, and Yang in Ref. [32].

[2]Regions of the multiverse may also (or instead) be described by quantum diffusion [53–55], i.e. eternal inflation may be driven by the potential energy of some light scalar field(s), the evolution of which is dominated by quantum fluctuations. Pockets form when the scalar field(s) fluctuate into a region of parameter space where classical evolution dominates, and slow-roll inflation ensues. In this case, the pocket geometry in general does not contain the global symmetry of those formed via bubble nucleation. Nevertheless, the curvature perturbation at the onset of slow-roll inflation is still typically order unity, and an analysis similar to that in this paper could be performed. On the other hand, models of inflation featuring quantum diffusion typically have very flat potentials and a large number of e-folds between the onset and end of classical slow-roll inflation. Therefore, in this paper we ignore this type of cosmological evolution.

is just one dominant vacuum, the de Sitter vacuum with the smallest decay rate. For our purposes it is sufficient to note that

$$\gamma \approx 3, \tag{6}$$

with corrections on the order of the exponentially suppressed decay rate of the dominant vacuum (specifically, the smallest-magnitude rate equation eigenvalue). As an example of this asymptotic scaling behavior, the number of bubbles of our type that nucleate between the time t and $t + dt$ has the form

$$dn \propto e^{\gamma t} dt. \tag{7}$$

This scaling behavior holds even when the multiverse contains regions governed by quantum diffusion (c.f. footnote [2]); for details see, for example, Ref. [57].

B. The geometry of pocket nucleation

We here provide some background on the geometry of bubble nucleation; this section is largely based on Ref. [46] (while this paper was in preparation, a similar analysis appeared in Ref. [32]). To begin, consider a bubble of our vacuum that nucleates at scale-factor time $t_{\rm nuc}$. The parent vacuum in which our bubble nucleates can be described by flat de Sitter coordinates with metric

$$ds^2 = -dt^2 + e^{2t}(dr^2 + r^2 d\Omega_2^2), \tag{8}$$

where t is the flat de Sitter time, defined so as to coincide with the scale-factor time in the parent vacuum, and $d\Omega_2^2 = d\theta^2 + \sin^2\theta d\phi^2$. We assume the parent vacuum has a larger vacuum energy than ours. The nucleation process is then as described in Ref. [41]: the bubble starts as a small three-sphere and expands at a rate that rapidly approaches the speed of light.

Inside the bubble, we take interest in the open FRW coordinates (τ, ξ), which are described by the metric

$$ds^2 = -d\tau^2 + \tilde{a}^2(\tau)(d\xi^2 + \sinh^2\xi d\Omega_2^2). \tag{9}$$

Here $\tilde{a}(\tau)$ is the scale factor within the bubble, which should not be confused with that outside the bubble. We define proper time τ such that $\tau = 0$ at the bubble wall. The coordinates (τ, ξ) are natural to an observer inside the bubble—surfaces of constant proper time τ have a constant energy density and a constant curvature term $1/\tilde{a}^2$, i.e. the Einstein field equation gives

$$H^2 - \frac{1}{\tilde{a}^2} = \frac{8\pi G}{3}\rho_{\rm total}. \tag{10}$$

Note that curves of constant ξ, θ, and ϕ define a congruence of comoving geodesics inside the bubble.

In order to obtain a simple relationship between the global geodesic congruence and that defined inside the bubble, we consider a simple model of bubble nucleation [46]. Specifically, we model the false-vacuum inflation of the parent vacuum, the tunneling event, and the subsequent evolution in the bubble (up to reheating) using a single scalar field φ, with potential $V(\varphi)$ (as illustrated in Fig. 1). Furthermore, we assume the tunneling barrier of V is such that $V(\varphi)$ is nearly the same before and after tunneling, and that gravitational effects of the bubble wall are negligible. Because of the symmetries of the tunneling instanton, the field φ emerges after tunneling with zero "velocity," $d\varphi/d\tau = 0$ [41]. Therefore, at very early times τ the geometry inside the bubble is approximately de Sitter.

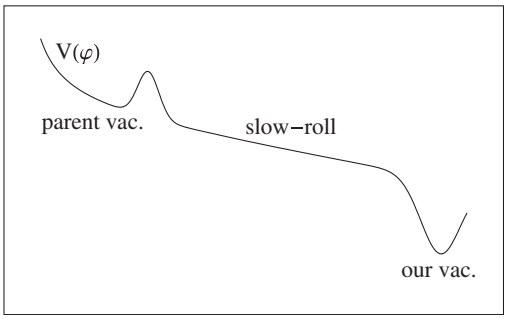

FIG. 1. The potential $V(\varphi)$ describing the parent vacuum, slow-roll inflation potential, and our vacuum.

Because the vacuum energy is nearly the same outside and just inside the bubble, and the geometry in both regions is de Sitter, constant r geodesics pass unaffected through the bubble wall. Thus, in this de Sitter region the global geodesic congruence and that inside the bubble are related by the usual relationship between flat and open de Sitter coordinates:

$$\begin{aligned} H_i t(\tau, \xi) &= \ln[\cosh(H_i\tau) + \sinh(H_i\tau)\cosh\xi], \\ H_i r(\tau, \xi) &= \frac{\sinh(H_i\tau)\sinh\xi}{\cosh(H_i\tau) + \sinh(H_i\tau)\cosh\xi}, \end{aligned} \tag{11}$$

where H_i is the Hubble rate of the parent vacuum. Note that H_i is not the Hubble rate at early times in the bubble, even though the energy density V is nearly the same in both regions. This is because of the curvature term in Eq. (10). Solving Eq. (10) in the limit $V(\varphi) \approx V(\varphi_i) = 3H_i^2/8\pi G$, one finds

$$\tilde{a}(\tau) = H_i^{-1}\sinh(H_i\tau), \tag{12}$$

(the singularity $a \to 0$ as $\tau \to 0$ is only a coordinate singularity). This solution holds as long as $V(\varphi)$ does not change significantly, i.e. as long as $H_i\tau \ll \sqrt{16\pi G}V/V'$, where the prime denotes φ differentiation [46].

After entering the de Sitter region just inside the bubble wall, geodesics of constant r (which are comoving in the parent vacuum) asymptote to the geodesics of constant ξ (which are comoving in the bubble), up to corrections of order $e^{-H_i\tau}$. See Fig. 2 for an illustration. We assume that we can map these geodesics onto each other with reasonable accuracy during the early de Sitter expansion, i.e. we assume there exists a time τ_i satisfying $1 \ll H_i\tau_i \ll \sqrt{16\pi G}V/V'$. The scale-factor time at τ_i is then given by

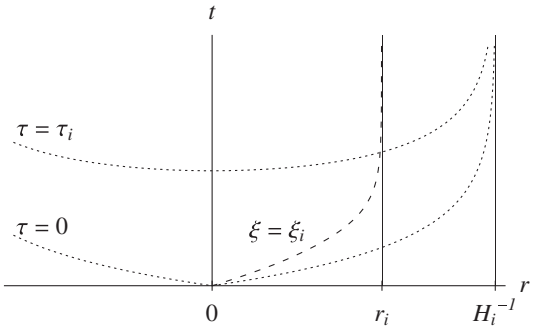

FIG. 2. The geometry near the bubble boundary.

$$t_i = t_{\rm nuc} + H_i\tau_i + 2\ln\cosh(\xi/2), \tag{13}$$

which is obtained by taking the limit $H_i\tau_i \gg 1$ of Eqs. (11).

After the proper time τ_i, the bubble expands through N_e e-folds of slow-roll inflation, reheats, and then undergoes big bang evolution. We will take interest in a reference class of observers who measure Ω_k^0 at the same FRW proper time, τ_0. We denote the number of e-folds of expansion along a constant-ξ geodesic from reheating to this time N_0. Then the scale-factor time at which these observers measure Ω_k^0 can be written

$$t_0 = t_{\rm nuc} + H_i\tau_i + 2\ln\cosh(\xi/2) + N_e + N_0. \tag{14}$$

Note that t_0 is a function of ξ. Thus, the scale-factor cutoff, which requires $t_0 \leq t_c$, implies a cutoff on the FRW coordinate ξ, $\xi \leq \xi_c$, with

$$\xi_c = 2\cosh^{-1}\exp\left[\frac{1}{2}(t_c - t_{\rm nuc} - H_i\tau_i - N_e - N_0)\right]. \tag{15}$$

The cutoff ξ_c in turn implies that the constant $\tau = \tau_0$ hypersurface on which Ω_k^0 is measured, Σ_0, is finite.

The number of observers that arise in the bubble before the cutoff t_c is proportional to the physical volume of Σ_0. More precisely, the number of observers is proportional to the matter density on Σ_0 times its physical volume. After inflation the matter density dilutes with cosmic expansion, so the number of observers can be taken to be proportional to the comoving volume of Σ_0 at reheating

$$V_* = 4\pi\tilde{a}^3(\tau_*)\int_0^{\xi_c}\sinh^2\xi d\xi, \tag{16}$$

where τ_* is the proper time of reheating. Note that the bubble scale factor at proper time τ_i is $\tilde{a}(\tau_i) \approx \frac{1}{2}H_i^{-1}e^{H_i\tau_i}$—this is Eq. (12) in the limit $H_i\tau \gg 1$. Thus, Eq. (16) can be written

$$V_* = \frac{\pi}{2}H_i^{-3}e^{3(H_i\tau_i+N_e)}\int_0^{\xi_c}\sinh^2\xi d\xi. \tag{17}$$

In Sec. III we take interest in the volume at thermalization, V_*, as well as the curvature parameter Ω_k^0, evaluated on the hypersurface Σ_0, as a function of N_e. The curvature parameter at τ_0 can be related to its value at any previous (proper) time using

$$\Omega_k^0 = \Omega_k^q(\tilde{a}_qH_q/\tilde{a}_0H_0)^2, \tag{18}$$

where the subscript 0 denotes quantities evaluated at τ_0, and q denotes quantities evaluated at some previous time. We set the previous time to be that of bubble nucleation, $\tau = 0$ in open FRW coordinates. From Eqs. (10) and (12), we see $\tilde{a}(\tau)H(\tau) \to 1$ and $\Omega_k(\tau) \to 1$ as $\tau \to 0$. During inflation the scale factor expands exponentially with time, while after inflation it is convenient to write the scale factor as a function of the temperature T, as opposed to the proper time τ. Assuming instantaneous reheating and conserving entropy in comoving volumes, the scale factor at temperature T can be written

$$\tilde{a}(T) = \frac{1}{2}H_i^{-1}e^{H_i\tau_i+N_e}\left(\frac{g_*T_*^3}{gT^3}\right)^{1/3}, \tag{19}$$

where T_* is the reheating temperature and g counts the effective number of degrees of freedom in thermal equilibrium (g_* being the corresponding quantity at the reheating temperature). We neglect $H_i\tau_i$ next to N_e in the exponent of Eq. (19), which allows us to write

$$\Omega_k^0 = \left(\frac{2H_ig_0^{1/3}T_0}{H_0g_*^{1/3}T_*}\right)^2e^{-2N_e}. \tag{20}$$

The error introduced by ignoring $H_i\tau_i$ can be offset by a small shift in the value of N_e; however, we treat N_e as an unknown, scanning parameter, and such a shift is not important to our results. To proceed, we make educated guesses at the unknown parameters in Eq. (20). First, note that according to our assumption of instantaneous reheating, the Hubble rate and temperature at reheating are related by $H_*^2 = (8\pi^3G/90)g_*T_*^4$. We consider H_i to be a factor of a few larger than H_*, take g_* to be on the order of a hundred, and guess $T_* \approx 10^{-4}G^{-1/2}$ (i.e. grand unified theory-scale reheating). Putting all this together gives

$$\Omega_k^0 \approx e^{123-2N_e}, \tag{21}$$

where we have also input the present temperature $T_0 = 2.34 \times 10^{-4}$ eV and Hubble rate $H_0 = 1.53 \times 10^{-33}$ eV. We comment on the effect of changing our guess of T_* at the end of Sec. III.

C. Structure formation in an open FRW universe

Anthropic selection in favor of structure formation may be an important effect modulating the distribution of Ω_k. Therefore, we take interest in the details of structure formation in universes in which Ω_k may deviate significantly from zero (the work here builds upon that of Refs. [11,46,47]). In this section, we describe the relevant aspects of structure formation by looking at the evolution within a single bubble like ours. In Sec. III, we incorporate these results into the complete picture involving a diverg-

ing number of bubbles that nucleate throughout the evolution of the multiverse.

In the context of estimating anthropic selection for structure formation, one often studies the asymptotic collapse fraction. This is because one is interested in *explaining*, say, the observed value of Λ, and one anticipates that observers like us could arise at times somewhat different than the present cosmic time, and in galaxies with mass somewhat different than that of the Milky Way (see, for example, Refs. [58,59]). If one were instead interested in the best possible *prediction* of Λ, one would use as much information as is relevant to constrain it [60]. In this case, we would take interest in the fraction of matter in halos with mass similar to that of the Milky Way, since it is in this halo that we perform the measurement.

We denote the collapse fraction into halos of mass greater than or equal to M_G at time τ as $F_c(M_G, \tau)$. The collapse fraction into only halos of mass equal to M_G is better known as the mass function (evaluated at M_G), and we denote this $F_m(M_G, \tau)$. The collapse fraction F_c can be approximated using the Press-Schechter formalism [61], which gives

$$F_c = \mathrm{erfc}\left[\frac{\delta_c}{\sqrt{2}\sigma_{\mathrm{rms}}(M_G, \tau)}\right]. \tag{22}$$

Here δ_c is the collapse density threshold—the amplitude reached by the linear evolution of an overdensity at the time when a nonlinear analysis would reveal that it has collapsed—and $\sigma_{\mathrm{rms}}(M_G, \tau)$ is the root-mean-square (rms) density contrast on the comoving scale enclosing a mass M_G and evaluated at proper time τ. The collapse density threshold δ_c is not constant in time when $\Omega_k \neq 0$, nor when $\Lambda \neq 0$; however it changes by less than 10% over the course of big bang evolution [11,62] and the collapse fraction F_c (as well as the mass function F_m) is well-approximated by taking $\delta_c = 1.69$.

According to the Press-Schechter formalism, the mass function F_m can be obtained by differentiation, $F_m = (dF_c/d\ln M_G)$—this corresponds to the distribution of halo masses at any given time. Note that the only M_G dependence of F_c comes from σ_{rms}. Meanwhile, the M_G dependence of σ_{rms} factors out of its time evolution, i.e.

$$\sigma_{\mathrm{rms}}(M_G, \tau) = \bar{\sigma}_{\mathrm{rms}}(M_G) G_\Omega(\tau), \tag{23}$$

where $\bar{\sigma}_{\mathrm{rms}}(M_G)$ is related to the rms primordial density contrast on comoving scales enclosing mass M_G. At fixed M_G, $d\sigma_{\mathrm{rms}}/d\ln M_G = (d\bar{\sigma}_{\mathrm{rms}}/d\ln M_G) G_\Omega \propto \sigma_{\mathrm{rms}}$, and so we write

$$F_m \propto \frac{1}{\sigma_{\mathrm{rms}}(M_G, \tau)} \exp\left[\frac{\delta_c^2}{2\sigma_{\mathrm{rms}}^2(M_G, \tau)}\right], \tag{24}$$

and interpret this as the mass fraction in halos with mass M_G. Both F_c and F_m are functions of σ_{rms}, and so we now turn to describing this quantity.

The factor $G_\Omega(\tau)$ in Eq. (23) is called the growth factor, and an integral expression for it may be obtained by analyzing the first order Einstein field equation [63]. It is convenient to first define a new time variable,

$$x = \rho_\Lambda/\rho_m \propto \tilde{a}^3(\tau), \tag{25}$$

where ρ_Λ is the energy density in cosmological constant, ρ_m is the matter density, and $\tilde{a}$ is the scale-factor [of the open FRW coordinates of the bubble, see Eqs. (9) and (10). The growth function is then

$$G_\Omega(x) \propto \sqrt{1 + \frac{1}{x} + \frac{k}{x^{2/3}}} \int_0^x \frac{y^{-1/6} dy}{(1 + y + k y^{1/3})^{3/2}}, \tag{26}$$

where the curvature term k is defined by matching onto the Einstein field equation,

$$H^2 = H_\Lambda^2 (1 + x^{-1} + k x^{-2/3}), \tag{27}$$

where again $H_\Lambda^2 \equiv 8\pi G \rho_\Lambda/3$. Thus, the curvature term k is related to Ω_k by

$$\Omega_k = \frac{k x^{1/3}}{1 + x + k x^{1/3}}. \tag{28}$$

In Eq. (27) we have ignored the presence of radiation in our Universe, since its effect on our analysis is negligible. Even with this simplification, Eq. (27) cannot be solved in closed form. Instead, the evolution of x with time is given by the integral expression

$$H_\Lambda \tau = \frac{1}{3} \int_0^x \frac{dz}{\sqrt{z^2 + z + k z^{4/3}}}. \tag{29}$$

This relation defines a function $\tau(x)$ relating the proper time in the bubble to the new time variable x. The function $\tau(x)$ can be obtained by numerical interpolation and (numerically) inverted to give $x(\tau)$.

The functions F_c and F_m are in a sense anthropic factors, as they are approximately proportional to the number of observers that arise in a fixed comoving volume of some bubble at (or before) some specified time. Note that we here use the term "anthropic factor" loosely, as we are only looking at a single bubble and the scale-factor cutoff will introduce an additional selection effect when we account for all of the bubbles in the multiverse. Nevertheless, it is worthwhile to study the distributions $F_c(\Omega_k)$ and $F_m(\Omega_k)$. Of course, both of these depend on the time at which they are evaluated. As we are ultimately interested in imposing a global time cutoff, we first evaluate F_c and F_m at a fixed proper time $\Delta\tau$ before the present "time" $x_0 = 2.88$. The rationale behind this is to allow sufficient time after a halo collapse for planet formation and the evolution of observers, while at the same time increasing predictive power by restricting attention to observers who perform the measurement of Ω_k at the same time that we do.

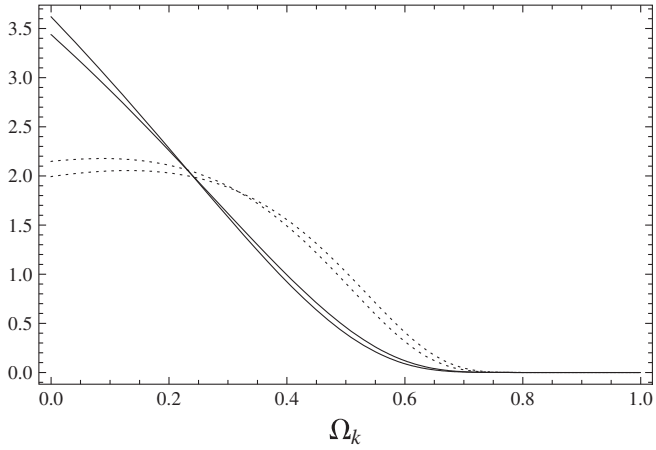

FIG. 3. The collapse fraction $F_c(\Omega_k)$ (solid line) and mass function $F_m(\Omega_k)$ (dotted line); see the text for details.

The resulting distributions $F_c(\Omega_k)$ and $F_m(\Omega_k)$ are displayed in Fig. 3, where we have used $M_G = 10^{12} M_\odot$, $M_\odot$ being the solar mass, and have chosen $\Delta\tau = 5 \times 10^9$ years. Alongside these are displayed the same distributions but ignoring the proper time lapse $\Delta\tau$, i.e. setting $\Delta\tau = 0$. We have normalized the distributions to integrate to unity. Here and throughout the paper we use WMAP-5 mean value parameters [50][3] and compute the rms density contrast on the scale M_G using Ref. [64] and the CMBFAST program. For both F_c and F_m, the curve with $\Delta\tau = 0$ is the one that is slightly higher at larger Ω_k. Note that the distributions do not depend significantly on the choice of $\Delta\tau$. For this reason, and because it dramatically simplifies our calculations, henceforth we set $\Delta\tau = 0$.

Figure 3 reveals that, although anthropic selection prevents an observer from measuring too large a value of Ω_k, it does not select values of Ω_k as small as the observational bound ($\Omega_k^0 \leq 0.013$ at 95% confidence level [50]) much more strongly than it selects values, say, 10 times larger than this. We return to this point in Sec. IV.

III. THE DISTRIBUTION OF Ω_k

We can now describe what value of Ω_k we might expect to measure, given certain assumptions about the multiverse. In any given bubble, the value of Ω_k is a function of the expansion history along the comoving geodesic passing through the spacetime point at which Ω_k is measured. This expansion history is well understood only during (a portion of) the big bang evolution following reheating. Although many factors contribute to the expansion history before this big bang evolution, we bundle our ignorance into a single parameter: the number of e-folds of slow-roll inflation in our bubble, N_e. This is to say, we make guesses at relevant quantities such as the scale of inflation and the reheating temperature (see the end of Sec. II B), and consider that our errors are offset by (small) changes in the number of e-folds N_e. The distribution of N_e is of course crucial to the analysis, yet in this aspect of the calculation that we must rely on a high degree of speculation.

As indicated from the onset of this paper, we consider our Uuniverse to be a thermalized bubble in an eternally inflating multiverse. Furthermore, we consider the multiverse to be populated by a landscape of vacua so large that we may consider the early dynamics of our bubble as independent of the low-energy physics that describes the subsequent big bang evolution. In this picture, we expect the value of N_e in our bubble to be typical of values across the multiverse, modulo any selection effects. To guess at this distribution, we follow FKRMS [47].

These authors consider the dominant contribution to N_e to come from the slow-roll of a single scalar field over an approximately linear potential,

$$V(\varphi) \approx V_0\left(1 - \frac{y}{\Delta}\varphi\right), \qquad \varphi_i \leq \varphi \leq \varphi_f, \tag{30}$$

where V_0, y, and $\Delta \equiv \varphi_f - \varphi_i$ are free parameters that are assumed to scan across the landscape, taking values between zero and one (in Planck units) with uniform probability distribution. The primordial density contrast can be calculated from Eq. (30), and is a function of the parameters V_0, y, and Δ. Since the primordial density contrast is known, we consider the slice of the landscape of $V(\varphi)$ for which it is fixed to the value we measure. The resulting distribution of N_e is [47]

$$dP_0(N_e) \propto N_e^{-4} dN_e, \tag{31}$$

where here the subscript "0" emphasizes that we have not yet accounted for all of the selection effects. Equation (31) is converted into a distribution of Ω_k^0 using Eq. (21), which gives

$$\frac{dP_0(\Omega_k)}{d\ln\Omega_k^0} \propto \left[61.5 - \frac{1}{2}\ln\Omega_k^0\right]^{-4} \equiv f(\Omega_k^0). \tag{32}$$

We now take into account the other selection effects, namely, the effect of the scale-factor measure over the multiverse and the effect of anthropic selection in favor of structure formation. Let us first write the result in a somewhat cumbersome form, in order to explain the various contributions, and then simplify it. The distribution of Ω_k^0 can be written

$$\frac{dP(\Omega_k^0)}{d\ln\Omega_k^0} \propto \lim_{t_c\to\infty} \int_{-\infty}^{t_c} e^{\gamma t_{\rm nuc}} dt_{\rm nuc} \times \int_0^{\xi_c} e^{3(H_i\tau_i + N_e)} \sinh^2\xi d\xi \times F_m(M_G, x_0) f(\Omega_k^0). \tag{33}$$

[3]The relevant values are $\Omega_\Lambda = 0.742$, $\Omega_m = 0.258$, $\Omega_b = 0.044$, $n_s = 0.96$, $h = 0.719$, and $\Delta^2_{\mathcal{R}}(k = 0.02\ \mathrm{Mpc}^{-1}) = 2.21 \times 10^{-9}$.

The integral on the second line is proportional to the total amount of matter on the hypersurface Σ_0, given by Eq. (17), while the mass function F_m selects for the fraction of matter that has collapsed into halos of mass M_G. Collectively, these terms are proportional to the number of observers like us in bubbles that nucleate at scale-factor time $t_{\rm nuc}$ [the dependence on $t_{\rm nuc}$ is in the limit of integration ξ_c, see Eq. (15)]. The first line of Eq. (33) integrates over all bubble-nucleation times $t_{\rm nuc}$, with the appropriate volume weighting coming from eternal inflation with the scale-factor measure, see, for example, Eq. (7). This integration ignores the very small probability that a given vacuum might decay during slow-roll inflation or big bang evolution up to the hypersurface Σ_0. Finally, the last term in the last line of Eq. (33) gives the distribution of Ω_k^0 coming from the dependence on the number of e-folds of slow-roll inflation, Eq. (32).

As explained in Sec. II C, we here use the mass function F_m instead of the collapse fraction F_c because we are interested in making a prediction, so we include as much relevant information as is practical—in this case that we live in a halo with mass equal to that of the Milky Way. Thus, we set $M_G = 10^{12} M_\odot$. Although the difference between F_c and F_m is conceptually relevant, Fig. 3 indicates that the two distributions differ at most by a factor of order unity, which does not significantly affect the anthropic constraints. Similarly, we evaluate the mass function at the present ratio of energy density in cosmological constant to that in matter, $x_0 = 2.88$.[4] One might wonder how the prediction of Ω_k is affected if we do not so strongly condition the calculation. We return to this question in Sec. IV.

To proceed, we first evaluate the inside integral over ξ. Note that all of the dependence on ξ is in the factor $\sinh^2\xi$. The integration can be performed analytically,

$$\int_0^{\xi_c} \sinh^2\xi d\xi = \sinh(2\xi_c) - 2\xi_c, \tag{34}$$

with ξ_c given by Eq. (15). It is convenient perform a variable redefinition,

$$z = t_c - t_{\rm nuc} - H_0\tau_0 - N_e - N_O, \tag{35}$$

and exchange integration over $t_{\rm nuc}$ for integration over z. The integration over z just gives a constant prefactor (here and below we use $\gamma = 3$). Dropping the other constant factors, Eq. (33) becomes

$$\frac{dP(\Omega_k^0)}{d\ln\Omega_k^0} \propto F_m(M_G, x_0) f(\Omega_k^0). \tag{36}$$

[4]We should include a time lapse $\Delta\tau$ to allow for planet formation and biological evolution after halo collapse. However, as mentioned in Sec. II C, this complicates the analysis but does not significantly affect the results, so for simplicity we neglect it.

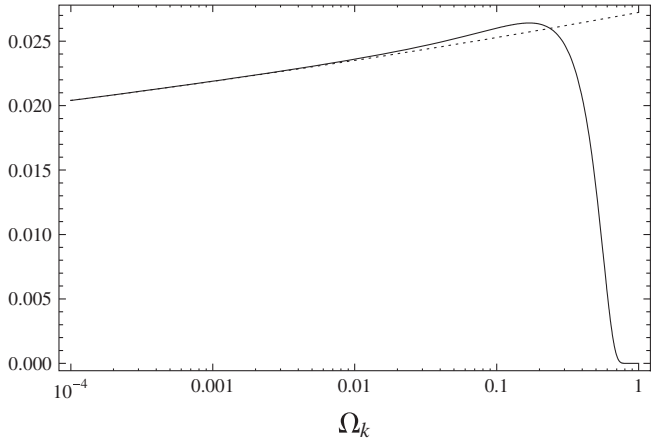

FIG. 4. The relevant portion of the distribution of Ω_k^0 (solid line), along with a simple approximation, Eq. (37) (dotted line).

Note that Eq. (36), which includes the effect of the scale-factor cutoff, is exactly what one would naively expect if the issue of measure were ignored.

The distribution equation (36) is displayed (in part) in Fig. 4. Interestingly, the distribution is quite flat all the way up to rather large values of Ω_k^0, falling off at $\Omega_k^0 \approx 0.6$. We know from CMB measurements that $\Omega_k^0 \leq 0.013$ [50] (for simplicity we take this 95% confidence level to be a hard bound), so to produce the best prediction we should cut the distribution at that value. The distribution in Fig. 4 is normalized as if this cut were in place, and the small amplitude of the distribution (~ 0.02) indicates that it has broad support over values of Ω_k^0 much smaller than those displayed in the figure. This can also be seen by examining the approximation,

$$\frac{dP(\Omega_k^0)}{d\ln\Omega_k^0} \sim \left[61.5 - \frac{1}{2}\ln\Omega_k^0\right]^{-4}, \tag{37}$$

which (after proper normalization) is very accurate for small Ω_k^0. As another illustration of how broad is the distribution, note that the median sits at about $10^{-16.5}$ (corresponding to about 80 e-folds of slow-roll inflation).

Because of the broad support of the distribution equation (37), it is most likely that Ω_k^0 is dominated by cosmic variance—which is of order 10^{-5} [48]—instead of the relic contribution calculated above. Nevertheless, it is exciting that the distribution of Ω_k^0 leaves reasonable hope for future detection. In particular, there is a 6% chance to measure $\Omega_k^0 \geq 10^{-3}$, and an 11% chance to measure $\Omega_k^0 \geq 10^{-4}$ (both of these percentiles are calculated using a distribution cut off at $\Omega_k^0 = 0.013$). These results are in agreement with the estimates made in Ref. [47].

Recall that our analysis guessed at certain cosmological parameters, for example, the reheating temperature, which was set at $T_* \approx 10^{-4} G^{-1/2}$ (c.f. the end of Sec. II C). As a quick check of the effect of our guesses, consider a very different guess at the reheating temperature,

$T_* \approx 10^{-16} G^{-1/2}$ (corresponding to TeV-scale reheating). For simplicity we keep our other guesses fixed. In this case, the quantity "123" appearing in Eq. (21) becomes about 68. Performing an analysis analogous to that above, we find there is a 10% chance to measure $\Omega_k^0 \geq 10^{-3}$, and an 18% chance to measure $\Omega_k^0 \geq 10^{-4}$. Decreasing T_* shifts the distribution of Ω_k toward larger values, but apparently the effect is not very strong. The most important factor determining our expectations for Ω_k is the distribution of N_e over the landscape.

IV. ANTHROPIC CONSIDERATIONS AND THE "PRIOR" DISTRIBUTION OF N_e

The calculation of the last section was made in the spirit of a prediction, and as such it was conditioned by certain details about our location in our universe, namely, that we inhabit a galaxy with Milky Way mass and perform our measurement at $x_0 = 2.88$. Taking a different perspective, we can ask under what conditions can the landscape picture explain why the curvature is observed to be as small as it is, $\Omega_k^0 \leq 0.013$. In this case, we consider ourselves observers belonging to a more general reference class, and ask what values of Ω_k typical observers in this reference class measure. We consider here the more general reference class to be observers in bubbles with the same low-energy physics as ours, the same value of the cosmological constant, and in galaxies like the Milky Way, however these observers can arise at any time over the course of bubble evolution.

To proceed in analogy to the calculation of Sec. III introduces a number of unnecessary complications. Instead, we follow the methods introduced in Ref. [31]. Specifically, we take as our "reference objects" not entire bubbles, but small patches of comoving volume, whose transverse boundaries are bubble walls (or the cutoff hypersurface at scale-factor time t_c). If these patches are sufficiently small in spacelike extent, they may be chosen so that both scale-factor time t and proper time τ are nearly constant over slicings of the patch. These patches, like any reference object, arise in the multiverse at a rate that scales like that of Eq. (7). Integrating over these patches is equivalent to taking as the reference objects entire bubbles (cut off at t_c), and integrating over bubble nucleation times, as was done in Sec. III.

The curvature parameter Ω_k is a function of the FRW proper time τ inside each bubble. Therefore, to calculate what values of Ω_k typical observers measure, one must know the density of these observers as a function of time. Alternatively, one can define a time-invariant quantity k, related to Ω_k, and count the total number of observers inhabiting bubbles with different values of k. We use

$$k = \left(\frac{\Omega_k^3}{\Omega_\Lambda \Omega_m^2}\right)^{1/3}, \tag{38}$$

which corresponds to the quantity k used in Eq. (27). Note that the observational bound $\Omega_k^0 \leq 0.013$ corresponds to $k \leq 0.035$ [50].

To begin the calculation, consider a spacetime volume that is bound from below by a small patch of some bubble wall at scale-factor time t_w. The number of observers in this volume is proportional to the collapse fraction evaluated at a proper-time cutoff τ_c, where τ_c is defined by the relation

$$t_c - t_w = N_e + \int_{\tau_*}^{\tau_c} H(\tau) d\tau = N_e + \ln\left[\frac{\tilde{a}(\tau_c)}{\tilde{a}(\tau_*)}\right], \tag{39}$$

where τ_* is the (proper) time of reheating and N_e is the number of e-folds of expansion between the bubble wall and reheating. As our notation indicates, we assume the latter expansion comes entirely from slow-roll inflation; i.e. we neglect the contribution coming from the initial curvature-dominated phase.

The number of observers in such a patch can then be approximated as proportional to

$$e^{3N_e} F_c(M_G, \tau_c), \tag{40}$$

where the exponential gives the volume expansion factor coming from slow-roll inflation, and the second term evaluates the collapse fraction at the proper-time cutoff. The collapse fraction counts matter collapsed into halos of mass M_G or greater; however, halos with mass greater than M_G at time τ_c had mass equal to M_G at some time $\tau < \tau_c$, so these halos contribute to our reference class. As we have already noted, one might instead evaluate F_c at some time $\Delta\tau$ before τ_c, in order to give time for galaxies and observers to evolve between the time of collapse and the proper-time cutoff. However, including this effect significantly complicates the calculation, whereas in Sec. II B we found that it does not significantly affect the collapse fraction. Therefore, we here neglect it.

Summing over all patches gives

$$\frac{dP(k)}{d\ln k} \propto \lim_{t_c \to \infty} \int_{-\infty}^{t_c} e^{3N_e + \gamma t_w} F_c(M_G, \tau_c) \tilde{f}(k) dt_w, \tag{41}$$

where as before we have neglected the small probability that a given vacuum may decay during slow-roll inflation or during big bang evolution. As was the case with Eq. (33), the exponential dependence on N_e is an illusion. Note that the cutoff τ_c corresponds to a cutoff x_c, where as before $x \equiv \rho_\Lambda/\rho_m$. Equation (39) gives $\ln x_c = 3(t_c - t_w - N_e) + \text{const}$, which can be used to change the variable of integration from t_w to x_c. This gives

$$\frac{dP(k)}{d\ln k} \propto \int_0^\infty x_c^{-2} F_c(M_G, x_c) \tilde{f}(k) dx_c, \tag{42}$$

where we have used $\gamma = 3$. Note that the prior distribution $\tilde{f}(k)$ factors out of the integration.

The argument of Eq. (42) contains a factor of x_c^{-2}. This factor induces the "youngness bias" of the scale-factor cutoff measure, which prefers bubbles that nucleate nearer

to the cutoff (for which x_c is smaller). As shown in Ref. [31], this bias is rather mild. It does not appear in the calculation of Sec. III, c.f. Eq. (36), because that calculation was performed at fixed x, $x = x_0$.

Whereas $f(\Omega_k^0)$ of Eq. (36) corresponds to the distribution of $\Omega_k(x)$ at fixed $x = x_0$, the function $\tilde{f}(k)$ of Eq. (42) corresponds to the distribution of k, which is independent of x. Using $T \propto 1/\tilde{a} \propto x^{-1/3}$ and Eqs. (20) and (38), we find

$$k = e^{124-2N_e}, \tag{43}$$

where the additional factors of Ω_Λ and Ω_m essentially change the 123 of Eq. (21) to "124." In the case $dP_0(N_e) \propto N_e^{-4} dN_e$, this gives the distribution

$$\tilde{f}(k) \equiv \frac{dP_0(k)}{d\ln k} \propto \left[62 - \frac{1}{2}\ln k\right]^{-4}. \tag{44}$$

In Fig. 5 we display $dP(k)/dk$, using Eq. (42) with $\tilde{f}(k)$ given by Eq. (44). As in Fig. 4, we have cropped the figure to more clearly illustrate the region of interest (the cropped portion very closely follows the distribution $dP_0(k)/dk$). The observationally acceptable region, $k \leq 0.035$, is indicated by shading. Clearly, values of k satisfying our observational bound are not atypical in the FKRMS landscape model of inflation; in fact 93% of observers measure k to satisfy this bound.

Although typical observers measure $k \leq 0.035$, note that anthropic selection for structure formation, which causes the distribution of k to fall off at large k, does not select for values of k satisfying the observational bound much more strongly than it selects for values, say, 10 times larger. This is more clearly illustrated if we plot the distribution $dP(N_e)/dN_e$—i.e. the distribution of the observed number of e-folds N_e—using a flat prior for N_e, in other words setting $dP_0(N_e)/dN_e =$ constant. This is done in Fig. 6. The observational bound on k, and a bound 10 times larger, are converted to the e-folds of inflation and represented by the shaded regions.

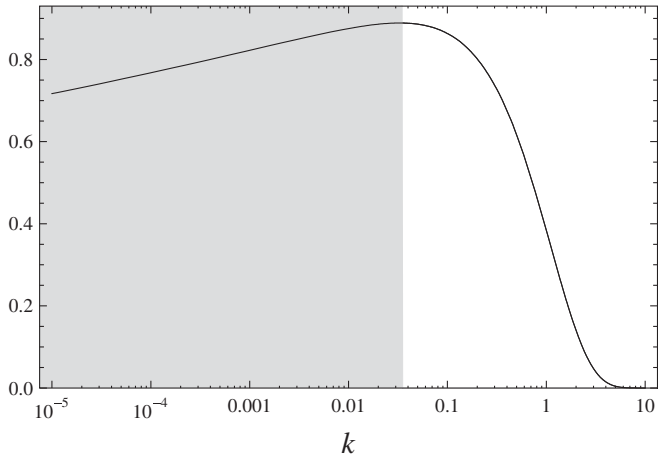

FIG. 5. The distribution $dP(k)/dk$; see the text for details. The present observationally acceptable region, $k \leq 0.035$, is indicated by shading.

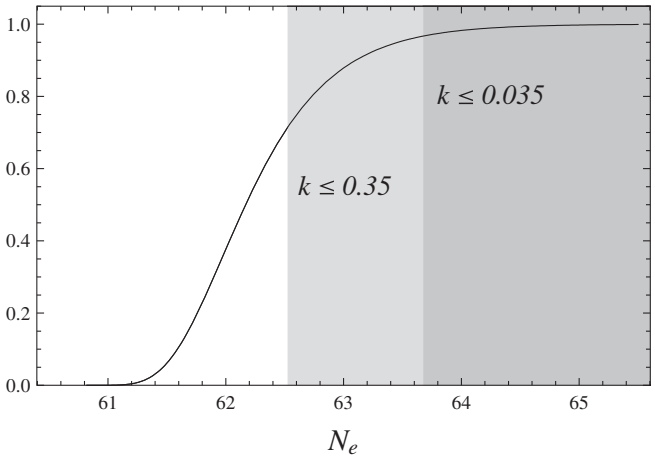

FIG. 6. The distribution $dP(N_e)/dN_e$ assuming a flat prior for N_e, i.e. $dP_0(N_e)/dN_e =$ constant. The shaded regions correspond to the observatinal bound $k \leq 0.035$, and a bound 10 times larger, translated to number of e-folds.

A flat prior for N_e is unrealistic, but it serves to illustrate the effect of anthropic selection. As expected, the distribution of N_e is exponentially suppressed for small values of N_e, where Fig. 6 reveals that in this context "small" means $N_e \lesssim 61$. The present observational bound, $k \leq 0.035$, corresponds to $N_e \geq 63.7$. Although the lower limit of this bound is not much larger than the anthropic cutoff at $N_e \approx 61$, k depends exponentially on N_e, and we can see from Fig. 6 that values of k over 10 times larger than the present bound are not strongly suppressed. This, in principle, allows us to exclude hypothetical landscape models of inflation, based on them predicting k to be larger than the observational bound.

In particular, if a hypothetical model of inflation in the landscape predicts a distribution of N_e that too strongly prefers smaller values of N_e, then it is possible for us to exclude this model based on the measurement $k \leq 0.035$. This is enticing because models of inflation in string theory tend to prefer a smaller number of e-folds of slow-roll inflation. On the other hand, it is important to recognize that in order to exclude a landscape model of inflation, we require a certain "fortuitous" shape to the prior distribution $dP_0(N_e)/dN_e$. For example, many classes of potentials will strongly prefer smaller values of N_e when N_e is small, but this region of the parameter space is not relevant to our observations, because values $N_e \lesssim 61$ are exponentially suppressed and do not contribute to the full distribution $dP(N_e)/dN_e$.

Let us illustrate this with an example. Consider a landscape model of inflation that predicts a power-law prior distribution of N_e,

$$dP_0(N_e) \propto N_e^{-\alpha} dN_e. \tag{45}$$

According to our assumptions, such a distribution is ruled out at greater than 95% confidence level when $\int_0^{0.035}(dP(k)/dk)dk < 0.025$, where $dP(k)/dk$ is here presumed to be normalized to unity. Performing the calculation, we find $\alpha \geq 114$ is ruled out. That only such a strong power-law dependence can be ruled out may be striking, but it is easy to understand in light of our above remarks. The observationally excluded region is, roughly speaking, $N_e < 64$; however anthropic selection suppresses all contributions from the interval $N_e < 61$. Therefore a landscape model of inflation is ruled out only if the prior distribution $dP_0(N_e)/dN_e$ has much more weight in the interval $61 \leq N_e \leq 64$ than in the interval $64 < N_e$. In the context of the power-law distribution of Eq. (45), we require

$$1 \ll \frac{\int_{61}^{64} N_e^{-\alpha} dN_e}{\int_{64}^{\infty} N_e^{-\alpha} dN_e} \approx \frac{3(\alpha - 1)}{64}. \tag{46}$$

Thus, roughly speaking, we expect to rule out power-law distributions only if $\alpha \gg 20$. The large power is explained by the fact that the prior distribution must have sharp behavior at large values of N_e.

Although it is hard to imagine how a landscape model of inflation could give such a strong power-law prior distribution of N_e, it is not implausible that a more realistic model of inflation, which could give a much more complicated prior distribution of N_e, could have the necessary sharp behavior at large N_e. Let us note, for instance, that potential energy barriers—as are necessary in the bubble-nucleation model we are considering—will give a sharp cutoff at large N_e.

Finally, we emphasize that the above analysis, which refers specifically to numbers like $N_e = 63.7$, etc., relies implicitly on a number of assumptions in addition to the form of the prior distribution of N_e, for example, the reheating temperature. These are described at the end of Sec. II B. Yet, different assumptions would merely shift the specific values of N_e mentioned above, and our conclusions would be unchanged.

V. CONCLUSIONS

Our Universe may be contained in one among a multitude of diverse bubbles in an eternally inflating multiverse. If the fundamental theory permits a landscape of metastable solutions, then in general one cannot make hard predictions about aspects of our Universe, but must instead understand it via conditional probability distributions. In such a multiverse, a diverging number of infinite-volume bubbles are formed, and weighing the various possibilities against each other requires regulation of these divergences. Different regulators give different observational predictions, and in this work we study the distribution of the curvature parameter Ω_k using one of the most promising regulators, the scale-factor cutoff.

In a large landscape, the vacuum of our bubble might be reached by tunneling from a number of different ''parent'' vacua. Then, depending on which parent vacuum our bubble nucleates, we in general expect different early universe dynamics, including different possibilities for the number of e-folds of slow-roll inflation N_e. In a very large landscape, as is expected from string theory, we also expect a large number of vacua with low-energy physics indistinguishable from our own. In this case, one expects a smooth distribution of possible values of N_e describing our bubble. One of the features of the scale-factor cutoff measure is that it does not reward bubbles for having a longer duration of slow-roll inflation. This raises the possibility that N_e may not be too much larger than is needed to pave the way for structure formation, and therefore that Ω_k^0 may be large enough to distinguish from the value expected from cosmic variance, $\sim 10^{-5}$.

Freivogel, Kleban, Rodriguez Martinez, and Susskind have proposed a toy model of inflation in the landscape, which gives a prior distribution of N_e of the form $dP_0(N_e) \propto N_e^{-4} dN_e$ (on the slice of the parameter space corresponding to a fixed primordial density contrast Q). Using the scale-factor cutoff measure, we find this distribution predicts a 6% chance to observe $\Omega_k^0 \geq 10^{-3}$, and an 11% chance to observe $\Omega_k^0 \geq 10^{-4}$, thus confirming the results of FKRMS [47].

Although in the FKRMS model of inflation in the landscape observers typically measure $k = (\Omega_k^3/\Omega_\Lambda \Omega_m^2)^{1/3}$ to satisfy our observational bound, $k \leq 0.035$, anthropic selection does not strongly suppress values of k over 10 times larger than this (when asking what typical observers measure, it is convenient to refer to the time-independent curvature term k rather than the time-dependent curvature parameter Ω_k). Thus, we may use the observed bound on k to rule out hypothetical landscape models of inflation that too strongly prefer smaller values of N_e.

Anthropic selection is not strong in the vicinity of the observational bound $k \leq 0.035$, however sufficiently large values of k are strongly suppressed. Put another way, with some assumptions about inflation $k \leq 0.035$ corresponds to $N_e \geq 63.7$. Anthropic selection is not strong in the vicinity of $N_e = 63.7$, but exponentially suppresses $N_e \lesssim 61$. This is to say a hypothetical model of inflation that very strongly prefers smaller values of N_e for $N_e \lesssim 61$ does not conflict with our observational bound, since this range of N_e is strongly anthropically suppressed. On the other hand, if a hypothetical model of inflation gives a prior distribution of N_e that strongly prefers N_e in the interval $61 \lesssim N_e < 63.7$, relative to it being in the interval $63.7 < N_e$, then such a model can be ruled out using our observational bound.

ACKNOWLEDGMENTS

We are grateful to Alan Guth and Alex Vilenkin for collaboration on parts of this work, and also thank Ken Olum for illuminating discussions. The work of ADS was supported in part by the INFN , and in part by the U.S.

Department of Energy (DoE) under Contract No. DE-FG02-05ER41360. MPS was supported in part by the U.S. National Science Foundation under Grant No. NSF 322.

APPENDIX A: LOCAL SCALE-FACTOR CUTOFF MEASURE

We here repeat the analysis of Secs. III and IV, but performing a cutoff on the local scale-factor time t' (see Sec. II A), where we use the prime to help distinguish the results here from those of the FRW scale-factor time t displayed throughout the main text. It is convenient to approach the problem in the manner of Sec. IV; that is we take as our reference objects small patches of comoving volume, with transverse boundaries corresponding to bubble walls (or the scale-factor cutoff hypersurface at t'_c). Again, if these patches are sufficiently small in their spacelike extent, the scale-factor time t' and the proper time τ are nearly constant over spacelike slicings of the patches. Analogous to Sec. IV, if we label each patch by the scale-factor time of reheating in the patch, t'_*, then such patches arise in the multiverse at a rate proportional to $e^{\gamma t'_*}$.

The scale-factor time t' probes expansion on infinitesimal scales. However, we take the number of observers to be proportional to the number of Milky Way-like galaxies, and we model such galaxies using spherical top-hat overdensities with mass $M_G = 10^{12} M_\odot$, so there is no need to probe scales smaller than the comoving volume that encloses mass M_G.[5] The probability that a comoving patch enclosing mass M_G contains an observer is then proportional to the probability that the smallest substructures within the patch began to collapse before the scale-factor time cutoff t'_c, and the entire region eventually collapses. (Recall that we have defined the scale-factor cutoff such that geodesics in collapsing regions are extended unless or until they hit a singularity.) This probability can be parametrized in terms of the spatial curvature of the patch at, say, the reheating time t'_*.

By Birkhoff's theorem, the evolution of a comoving patch enclosing a spherical top-hat overdensity is equivalent to that of a closed FRW universe with field equation

$$(\dot{y}/3y)^2 = H_\Lambda^2 (1 + y^{-1} - \kappa y^{-2/3}). \tag{A1}$$

The "local scale-factor cube root" y is defined so as to coincide with the "bubble scale-factor cube root" x of Eq. (27) [c.f. Eq. (25)] at early times. The total spatial curvature κ is the sum of the bubble curvature k (coming from the global bubble geometry) and the primordial curvature perturbation $\mathcal{R}$ (coming from quantum fluctuations during inflation). We define $\mathcal{R}$ to be positive for overdensities, so that

$$\kappa = \mathcal{R} - k. \tag{A2}$$

The spherical overdensity will turn around and begin to collapse before the scale-factor time cutoff t'_c only if the curvature exceeds some minimum value $\kappa_{\min}(t'_c, t'_*)$. For a bubble with a given value of k, the probability for this to occur is

$$\begin{aligned} \mathcal{A}(k; t'_c, t'_*) &\propto \int_{\kappa_{\min}}^{\infty} \exp\left[-\frac{(\kappa + k)^2}{\mathcal{R}_{\rm rms}^2}\right] d\kappa \\ &\propto \operatorname{erfc}\left[\frac{\kappa_{\min}(t'_c, t'_*) + k}{\sqrt{2}\mathcal{R}_{\rm rms}}\right], \end{aligned} \tag{A3}$$

where we assume $\mathcal{R}$ has a Gaussian distribution with rms value $\mathcal{R}_{\rm rms}$. As our notation suggests, $\mathcal{A}$ can be interpreted as an anthropic factor, giving the probability that a given patch contains an observer. The probability to observe a given value of k is thus

$$\frac{dP(k)}{d\ln k} \propto \lim_{t'_c \to \infty} \int_{-\infty}^{t'_c} \mathcal{A}(k; t'_c, t'_*) \tilde{f}(k) e^{\gamma t'_*} dt'_*, \tag{A4}$$

where, as in Eq. (44), $\tilde{f}(k)$ is the (logarithmic) distribution of k among universes with big bang evolution like ours, and $e^{\gamma t'_*}$ is proportional to the number of patches at scale-factor time t'_*.

It is left to solve for $\kappa_{\min}(t'_c, t'_*)$. First note that a spherical overdensity described by Eq. (A1) turns around and begins to collapse when $\dot{y} = 0$, or when $1 + y^{-1} - \kappa y^{-2/3} = 0$. Thus we can write

$$\kappa(y_{\rm turn}) = y_{\rm turn}^{-1/3}(1 + y_{\rm turn}). \tag{A5}$$

Meanwhile, $\kappa_{\min}$ is simply the value of κ for which $t'_c - t'_* = (1/3)\ln(y_{\rm turn}/y_*)$, where y_* is the local scale factor at the time of reheating. (Here we use the definition of scale-factor time, $t' = \ln a$, along with $y \propto a^{1/3}$.) Thus we can write

$$\kappa_{\min}(t'_c, t'_*) = y_*^{-1/3} e^{t'_* - t'_c}[1 + y_* e^{3(t'_c - t'_*)}]. \tag{A6}$$

The distribution of observed values of the bubble curvature k is obtained by combining Eq. (A4) with Eq. (A3) and (A6). The resulting expression is simplified if we change the integration variable from t'_* to $y_{\rm turn} = y_*^{1/3} e^{t'_c - t'_*}$. Then we can write

$$\frac{dP(k)}{d\ln k} \propto \int_{y_*}^{\infty} \operatorname{erfc}\left[\frac{1 + k y_{\rm turn} + y_{\rm turn}^3}{\sqrt{2}\mathcal{R}_{\rm rms} y_{\rm turn}}\right] \frac{\tilde{f}(k)}{y_{\rm turn}^4} dy_{\rm turn}, \tag{A7}$$

where we have used $\gamma = 3$. It makes no difference if we

[5] Realistically, structure formation is hierarchical: small scales turn around and collapse before larger scales. When the region surrounding a given geodesic collapses, its scale-factor time becomes frozen. Thus, it would seem we cannot ignore structure formation on such small scales. However, whether or not any observers arise in some small collapsed structure depends on whether that structure combines with others to form a larger structure—ultimately a large galaxy. We model the requirement that small structures coalesce into larger ones as equivalent to requiring that structure formation occurs on the largest necessary scale, using a spherical top-hot model for the initial overdensity.

simply set $y_* \to 0$ in the lower limit of integration. This expression corresponds to the analogue of Eq. (42), but for the local scale-factor time t', as opposed to the FRW scale-factor time t. $\mathcal{R}_{\rm rms}$ is the rms primordial curvature perturbation on comoving scales enclosing mass M_G—it is related to, say, the rms density contrast $\sigma_{\rm rms}$ by

$$\mathcal{R}_{\rm rms} = (5/3)\sigma_{\rm rms}(M_G, \tau_F)x_F^{-1/3}, \qquad \text{(A8)}$$

where the quantities on the right-hand side are evaluated at some fiducial time τ_F during matter domination, i.e. before vacuum energy or curvature become significant. [This relation is obtained from matching the linearized Einstein field equation onto Eq. (A1).]

Figure 7 displays $dP(k)/d\ln k$ using the scale-factor cutoff measure for both scale-factor time t' and scale-factor time t. We use Eq. (44) to determine $\tilde{f}(k)$ for clear comparison, and the shaded region indicates the bound $k \leq 0.035$. As advertised in the Introduction, the two definitions of scale-factor time give qualitatively similar results, however the anthropic suppression of large values of k kicks in at larger k when using the locally-defined scale-factor time t'. The two distributions are very similar for k less than the observed bound, indicating that the predictions of Sec. III are essentially unchanged when using the local scale-factor time. On the other hand, since the local scale-factor time measure permits larger values of k before strong anthropic suppression, if this is the correct measure then it would be somewhat easier (than indicated in Sec. IV) to rule out landscape models of inflation that prefer smaller values of N_e.

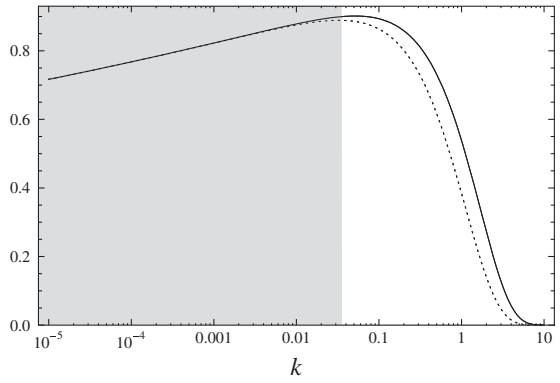

FIG. 7. The distribution $dP(k)/dk$ using scale-factor time t' (solid line) and t (dashed line); see text for details. The normalizations are chosen for clear comparison, while the shaded region indicates the observed bound $k \leq 0.035$.

[1] S. Winitzki, Lect. Notes Phys. **738**, 157 (2008).
[2] A. H. Guth, Phys. Rep. **333-334**, 555 (2000); J. Phys. A **40**, 6811 (2007).
[3] A. Linde, Lect. Notes Phys. **738**, 1 (2008).
[4] A. Vilenkin, J. Phys. A **40**, 6777 (2007).
[5] A. Aguirre, S. Gratton, and M. C. Johnson, Phys. Rev. Lett. **98**, 131301 (2007).
[6] A. D. Linde and A. Mezhlumian, Phys. Lett. B **307**, 25 (1993).
[7] A. D. Linde, D. A. Linde, and A. Mezhlumian, Phys. Rev. D **49**, 1783 (1994).
[8] J. Garcia-Bellido, A. D. Linde, and D. A. Linde, Phys. Rev. D **50**, 730 (1994); J. Garcia-Bellido and A. D. Linde, Phys. Rev. D **51**, 429 (1995); **52**, 6730 (1995).
[9] A. Vilenkin, Phys. Rev. Lett. **74**, 846 (1995).
[10] A. Vilenkin, Phys. Rev. D **52**, 3365 (1995).
[11] J. Garriga, T. Tanaka, and A. Vilenkin, Phys. Rev. D **60**, 023501 (1999).
[12] A. Vilenkin, Phys. Rev. Lett. **81**, 5501 (1998); V. Vanchurin, A. Vilenkin, and S. Winitzki, Phys. Rev. D **61**, 083507 (2000).
[13] J. Garriga, D. Schwartz-Perlov, A. Vilenkin, and S. Winitzki, J. Cosmol. Astropart. Phys. 01 (2006) 017.
[14] R. Easther, E. A. Lim, and M. R. Martin, J. Cosmol. Astropart. Phys. 03 (2006) 016.
[15] R. Bousso, Phys. Rev. Lett. **97**, 191302 (2006); R. Bousso, B. Freivogel, and I. S. Yang, Phys. Rev. D **74**, 103516 (2006).
[16] L. Susskind, arXiv:0710.1129.
[17] A. Linde, J. Cosmol. Astropart. Phys. 01 (2007) 022.
[18] A. Linde, J. Cosmol. Astropart. Phys. 06 (2007) 017.
[19] V. Vanchurin, Phys. Rev. D **75**, 023524 (2007).
[20] S. Winitzki, Phys. Rev. D **78**, 043501 (2008).
[21] J. Garriga and A. Vilenkin, J. Cosmol. Astropart. Phys. 01 (2009) 021.
[22] A. Linde, V. Vanchurin, and S. Winitzki, J. Cosmol. Astropart. Phys. 01 (2009) 031.
[23] R. Bousso, Phys. Rev. D **79**, 123524 (2009).
[24] A. D. Linde, D. A. Linde, and A. Mezhlumian, Phys. Lett. B **345**, 203 (1995).
[25] R. Bousso, B. Freivogel, and I. S. Yang, Phys. Rev. D **77**, 103514 (2008).
[26] B. Feldstein, L. J. Hall, and T. Watari, Phys. Rev. D **72**, 123506 (2005);
[27] J. Garriga and A. Vilenkin, Prog. Theor. Phys. Suppl. **163**, 245 (2006).
[28] M. L. Graesser and M. P. Salem, Phys. Rev. D **76**, 043506 (2007).
[29] M. Tegmark and M. J. Rees, Astrophys. J. **499**, 526 (1998).
[30] L. J. Hall, T. Watari, and T. T. Yanagida, Phys. Rev. D **73**, 103502 (2006).
[31] A. De Simone, A. H. Guth, M. P. Salem, and A. Vilenkin, Phys. Rev. D **78**, 063520 (2008).
[32] R. Bousso, B. Freivogel, and I. S. Yang, Phys. Rev. D **79**, 063513 (2009).
[33] A. De Simone, A. H. Guth, A. Linde, M. Noorbala, M. P.

Salem, and A. Vilenkin, arXiv:0808.3778.
[34] M. Rees, *Before the Beginning* (Addison-Wesley, Reading, 1997) p. 221.
[35] A. Albrecht and L. Sorbo, Phys. Rev. D **70**, 063528 (2004); see also A. Albrecht, in *Science and Ultimate Reality*, edited by J. D. Barrow, P. C. W. Davies, and C. L. Harper (Cambridge University Press, Cambridge, 2003).
[36] L. Dyson, M. Kleban, and L. Susskind, J. High Energy Phys. 10 (2002) 011.
[37] D. N. Page, J. Korean Phys. Soc. **49**, 711 (2006).
[38] D. N. Page, J. Cosmol. Astropart. Phys. 01 (2007) 004.
[39] D. N. Page, Phys. Rev. D **78**, 063535 (2008).
[40] R. Bousso and B. Freivogel, J. High Energy Phys. 06 (2007) 018.
[41] S. R. Coleman and F. De Luccia, Phys. Rev. D **21**, 3305 (1980).
[42] K. M. Lee and E. J. Weinberg, Phys. Rev. D **36**, 1088 (1987).
[43] R. Bousso, R. Harnik, G. D. Kribs, and G. Perez, Phys. Rev. D **76**, 043513 (2007).
[44] B. Bozek, A. J. Albrecht, and D. Phillips, Phys. Rev. D **80**, 023527 (2009).
[45] R. Bousso and S. Leichenauer, Phys. Rev. D **81**, 063524 (2010).
[46] A. Vilenkin and S. Winitzki, Phys. Rev. D **55**, 548 (1997).
[47] B. Freivogel, M. Kleban, M. Rodriguez Martinez, and L. Susskind, J. High Energy Phys. 03 (2006) 039.
[48] T. P. Waterhouse and J. P. Zibin, arXiv:0804.1771.
[49] M. Vardanyan, R. Trotta, and J. Silk, Mon. Not. R. Astron. Soc. (to be published).
[50] J. Dunkley *et al.* (WMAP Collaboration), Astrophys. J. Suppl. Ser. **180**, 306 (2009); E. Komatsu *et al.* (WMAP Collaboration), Astrophys. J. Suppl. Ser. **180**, 330 (2009).
[51] J. R. Gott, Nature (London) **295**, 304 (1982).
[52] P. J. Steinhardt, in *The Very Early Universe*, edited by G. W. Gibbons, S. W. Hawking, and S. T. C. Siklos (Cambridge University Press, Cambridge, 1983).
[53] A. Vilenkin, Phys. Rev. D **27**, 2848 (1983).
[54] A. D. Linde, Phys. Lett. B **175**, 395 (1986).
[55] A. A. Starobinsky, in *Field Theory, Quantum Gravity and Strings*, edited by H. J. De Vega and N. Sanchez, Lecture Notes in Physics (Springer, Berlin, 1986) p 381.
[56] D. Schwartz-Perlov and A. Vilenkin, J. Cosmol. Astropart. Phys. 06 (2006) 010.
[57] S. Winitzki and A. Vilenkin, Phys. Rev. D **53**, 4298 (1996).
[58] H. Martel, P. R. Shapiro, and S. Weinberg, Astrophys. J. **492**, 29 (1998).
[59] M. Tegmark, A. Aguirre, M. Rees, and F. Wilczek, Phys. Rev. D **73**, 023505 (2006).
[60] J. Garriga and A. Vilenkin, Phys. Rev. D **77**, 043526 (2008).
[61] W. H. Press and P. Schechter, Astrophys. J. **187**, 425 (1974); J. M. Bardeen, J. R. Bond, N. Kaiser, and A. S. Szalay, Astrophys. J. **304**, 15 (1986).
[62] P. B. Lilje, Astrophys. J. **386**, L33 (1992); M. Tegmark, A. Vilenkin, and L. Pogosian, Phys. Rev. D **71**, 103523 (2005).
[63] D. J. Heath, Mon. Not. R. Astron. Soc. **179**, 351 (1977).
[64] U. Seljak and M. Zaldarriaga, Astrophys. J. **469**, 437 (1996).